ACS APPLIED MATERIALS & INTERFACES

Research Article

www.acsami.org

TiO_2 Nanotube-Based Dye-Sensitized Solar Cell Using New Photosensitizer with Enhanced Open-Circuit Voltage and Fill Factor

W. Sharmoukh[†] and Nageh K. Allam*[,‡,§]

[†]Department of Inorganic Chemistry and [‡]Department of Physical Chemistry, National Research Center, Dokki, Cairo 12622, Egypt

[§]Energy Materials Laboratory (EML), School of Sciences and Engineering, The American University in Cairo, New Cairo 11835, Egypt

ABSTRACT: We report the synthesis and characterization of a high molar extinction coefficient ruthenium complex sensitizer (Ru (6,6′-$(COOEt)_2$-2,2′-bpy)$_2(Cl)_2$). In conjugation with TiO_2 nanotube arrays as a photoactive material and iodine/iodate redox electrolyte, we fabricated efficient dye-sensitized solar cell device showing a conversion efficiency of 3.94% measured under the air mass 1.5 global (AM1.5G) sunlight. The solar cell device showed a reasonably high open circuit voltage (0.74 V) as well as a fill factor of 0.63.

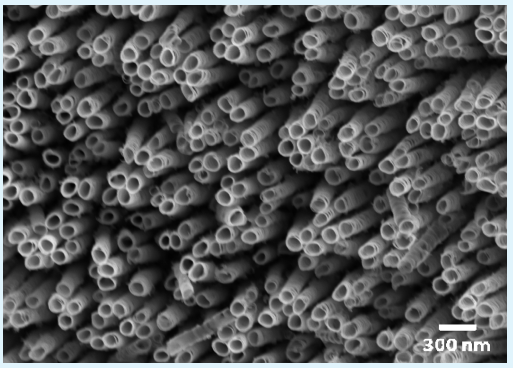

KEYWORDS: *Ru complexes, bipyridine, dye-sensitized solar cell, open-circuit voltage*

1. INTRODUCTION

With the looming energy crisis and the depletion of petroleum and natural-gas reserves, numerous ways have been investigated to convert the solar radiation directly into electrical power or chemical fuel.[1] However, the capital cost of such devices is still inconvenient for large-scale applications.

Solar cells based on dye-sensitized nanocrystalline TiO_2 have attracted considerable attention due to their high incident photon-to-current conversion efficiency (IPCE) presenting the opportunity of low-cost conversion of solar energy into electricity.[2] The ongoing research in dye-sensitized solar cells (DSSCs) is focusing on the optimization of all cell components; namely, the photoactive material (TiO_2), the dye and the redox electrolyte.[3]

The development of sensitizers, with spectral sensitivity over a wide region of the solar spectrum that enable efficient conversion of light, is a research field of great activity. In particular, ruthenium-based complexes have been used extensively as sensitizers.[4,5] Ruthenium (Ru) metal has been particularly chosen for a number of reasons:[6] (1) it has octahedral geometry that enable the introduction of specific ligands in a controlled manner; (2) it possesses various stable and accessible oxidation states; (3) it forms very inert bonds with imine nitrogen centers. In this regard, ruthenium polypyridyl complexes, of the type $[RuL_2(X)_2]$, (where L=4,4′-dicarboxylic acid-2,2′-bipyridine and 5,5′-dicarboxylic acid-2,2′-bipyridine; X= (Cl^-, CN^- and NCS^-) have been reported.[7,8] The lowest metal-to-ligand charge transfer (MLCT) absorption maxima of $[RuL_2(NCS)_2]$ complex (L = 2,2′-bipyridine) in ethanol was reported to be located at 510 nm.[7] Substituting two carboxylic acid groups at the 4,4′-position resulted in a red shift of the MLCT maxima to 535 nm.[8] However, substitution at the 5,5′-position shifted the maxima further into the red to 580 nm.[8] The enhanced red response of complexes containing the 5,5′-dicarboxylic acid was related to the decrease in the energy of the π^*-orbitals.[9] Despite this enhancement in the MLCT maxima, the IPCE of complexes having the 5,5′-dicarboxylic acid ligands was found to be lower than the 4,4′-dicarboxylic acid counterparts.[8] The low efficiency of the 5,5′-dicarboxylic acid-containing sensitizers was rationalized in terms of low excited state redox potentials.[9] These results highlight the influence of the position of the carboxylate groups on the MLCT transitions and consequently on the efficiency of such complexes as sensitizers. To this end, it seems that the 6,6′-dicarboxylic acid analogues ligands have not yet been investigated, which may present a new and completely different behavior of Ru-based sensitizers. Herein, we investigate the synthesis and use of such ligands.

Regarding the photoactive semiconducting material, the vertically oriented TiO_2 nanotube arrays, recently fabricated by anodization of titanium foil, are now the focus of research in solar energy conversion[10−15] among other applications.[16−20] For DSSCs, the properties of interest include the large internal surface area, enhanced optical absorption due to scattering effects, and lower recombination losses. Preliminary studies of ordered one-dimensional (1D) architectures including TiO_2 nanotubes and nanowires have indicated that, while the electron transport time is similar to that reported for dye

Received: June 18, 2012
Accepted: July 16, 2012
Published: July 16, 2012

   dx.doi.org/10.1021/am301089t | ACS Appl. Mater. Interfaces 2012, 4, 4413−4418

sensitized solar cells made from TiO_2 nanoparticles, the electron recombination time is much larger than for nanoparticulate electrodes resulting in improved charge collection efficiencies.[21,22] In comparison to ordered nanowire electrodes, nanotubes have significantly larger surface area because of the availability of both the internal and the external area of the nanotubes for dye coating.[23,24]

In this paper, we report a reliable strategy to combine the advantages of both components; namely the sensitizer and the photoactive semiconductor material. Particularly, we report the preparation and purification of new cis-ruthenium complexes with coordinated bipyridine-6,6′-dicarboxylate ligand and their use as sensitizers for TiO_2 nanotube arrays in a DSSC device.

2. EXPERIMENTAL SECTION

2.1. Materials and Apparatus. 2,2′-Bipyridine, mCPBA m-chloroperbenzoic acid and $RuCl_3{\cdot}H_2O$ were purchased from Aldrich Chemical Company, Inc., and used as supplied. Benzoyl chloride, potassium cyanide and sodium hydroxide were purchased from TCI (Japan). Methanol, ethanol, chloroform (Aldrich), and methylene chloride (TCI) were freshly distilled before use. ^1H and ^{13}C NMR spectra were recorded on a Varian 300 MHz spectrometer. High resolution mass spectra of new compounds were obtained using a Jeol JMS 700 spectrometer.

2.2. Preparation of Ligand. *2.2.1. 2,2′- Bipyridine-N,N′-dioxide.* 2, 2′- bipyridine (4g, 25.61 mmol) was dissolved in 50 ml Chloroform. mCPBA m-chloroperbenzoic acid (22.1 g, 64.03 mmol) dissolved in 200 ml Chloroform was added slowly (4 h) to this solution at zero temperature. After the completion of addition, the solution was stirred for another 2 days. The reaction was filtered off and quenched by the addition of methanol for one day. The precipitate is then filtered and dried at room temperature. (Yield 92 %)

^1H NMR (200 MHz, D_2O, ppm): 8.31- 8.27(d, 2H), 7.67-7.54(m, 6 H);

$^{13}CNMR$ (100 MHz, D_2O, ppm) 139.69, 137.60, 129.23, 126.75, 126.31

2.2.2. 6,6′-Dicyano-2,2′-bipyridine. 2,2′-Bipyridine-N,N′-dioxide (6g, 31.88 mmol) and potassium cyanide (12.3g, 189 mmol) were dissolved in 100 ml water. Methylene chloride (40 ml) and benzoyl chloride (15.69g, 111.6 mmol) were added slowly (3 h) to this solution at zero temperature. After that the reaction mixture was stirred for 4 h. The solution was filtered and quenched by ethanol for 1 day. The precipitate is filtered and dried at room temperature, with the obtained yield being 75%

^1H NMR (200 MHz, $CDCl_3$, ppm): 8.74-8.69(dd, 2H), 8.06–7.98(t, 2H), 7.79–7.75(dd, 2H); $^{13}CNMR$ (100 MHz, $CDCl_3$, ppm) 153.83, 138.78, 131.48, 129.01, 123.88, 116.24. Elem. Anal. Found: C, 69.95; H, 2.83; N, 27.39%. Theoretical: 69.90; H, 2.93; N, 27.17%).

2.2.3. 6,6′-Bis(ethoxycarbonyl)-2,2′-bipyridine. 6,6′-Dicyano 2,2′-bipyridine (5 g, 24.25 mmol) was dissolved in 80 mL of ethanol and 34 mL of sulfuric acid was added slowly to the solution. The reaction mixture heated to reflux for 1 day. The solution poured over 100 g of ice and stirred for 2 h, then extracted by methylene chloride. The solution is washed with brine three times and dried over magnesium sulfate anhydrous and reduced to yellowish-white solid (85%).

^1H NMR (200 MHz, $CDCl_3$, ppm) 8.79–8.74(dd, 2H), 8.16–8.12(dd, 2H), 8.02– 7.94)(t, 2H), 4.55–4.44(q, 4H), 1.50–1.43(t, 6H); $^{13}CNMR$ (100 MHz, CDCl3, ppm) 163.31, 153.63, 146.01, 136.18, 123.57, 122.84, 60.04. Elem. Anal. Found: C, 64.22; H, 5.37; N, 9.54%. Theoretical; C, 63.99; H, 5.37; N, 9.33%).

2.2.4. Preparation of 6,6′-Carbomethoxy-2,2′-bipyridine [$(COOCH_3)_2$bpy]:-. 6,6-bis(cyanomethyl)-2.2′-bipyridine(3g, 14.5 mmol) was dissolved in 70 mL of distilled methanol and 25 mL of sulfuric acid was added slowly. The reaction mixture was refluxed for 24 h. Consequently, the solution was poured onto 30 g of ice water. The solution was extracted with ethylene chloride, washed with brine and dried over magnesium sulfate anhydrous. The solution was concentrated to dryness using rotary evaporator to give white-yellow yield (80%).

^1H NMR (200 MHz, $CDCl_3$): δ 4.01(CH3), 8.01(t, J = 0.8 Hz, 2H), 8.16(d, J = 4.6 Hz, 2H), 8.74(d, J = 1.4 Hz, 2H). $^{13}CNMR$ (100 MHz, CD_3OD): δ52.87, 124.72, 125.36, 137.954, 147.36, 155.29, and 165.49 .GC-MS (EI) 272.0(M^+)

2.2.5. Preparation of 6,6′-Dicarboxy-2,2′-bipyridine, dcbpy. 6.6′-Dis(ethoxycarbonyl-2.2′-bipyridine(0.86 mg, 2.8 mmol) was dissolved in 40 mL of ethanol and sodium hydroxide (0.45 mg,11.45 mmol) was added. The reaction mixture was heated and refluxed for 4 h, after which the solution was poured onto 30 mL of water and acidified with HCl. The precipitate was filtered off and dried at room temperature.

^1H NMR (200 MHz, DMSO): δ 8.21–8.13 (4H), 8.7(d, 2H), $^{13}CNMR$ (100 MHz, DMSO): δ 124.31, 125.40, 139.09, 148.07, 154.51, and 166.05. Elem. Anal. for $C_{12}H_8N_2O_4{\cdot}1/2H_2O$. Found: C, 57.36; H, 3.25; N, 11.09. Theoretical: C, 57.36; H, 3.25; N, 11.09

2.2.6. Preparation of Complexes. Solid $RuCl_3{\cdot}3H_2O$ powder (0.250 g, 0.0.957 mM) was dissolved in 75 mL of ethanol under a N_2 atmosphere. After stirring for 20 min, 0.632 g (2.11 mM) of 6, 6′-$(COOEt)_2$-2,2′-bpy ligand was added. The reaction mixture was refluxed in darkness for 6 h with continuous stirring. After this period heating was suspended, and the solution kept under stirring for a further 1 h. The reaction flask was allowed to cool to room temperature and was filtered through sintered glass crucible. The ethanol solvent was evaporated completely under vacuum. The resulting solid product is washed with 75 ml of 2 M HCl. consequently, the solid is dissolved in ethanol then precipitated by adding diethyl ether.

^1H NMR (400 MHz,CD_3OD): δ 1.2 (d, CH3, J = 6 Hz, J =0.8 Hz, 6H), 1.4 (d, CH3′, J = 6.4 Hz; J =0.8, 6H), 3.6 (CH2, J = 6 Hz; J = 0.8, 4H), 4.5 (CH2′, J = 6.4 Hz; J = 0.8 Hz, 4H), 8.2(dd, J= 7.6 Hz, 8H), 8.7 (dd, J = 7.6 Hz, 4H). $^{13}CNMR$ (100 MHz, CD_3OD): δ 14.74, 18.54 (J = 5.3 Hz), 58.43, 63.40, 126.27, 126.82, 140.29, 148.5 (J = 14.4 Hz), 156.1(J = 14.4 Hz), 166.79.

2.2.7. Preparation of TiO_2 Nanotube Arrays. Highly-ordered TiO_2 nanotube arrays were fabricated via the anodization of titanium foil (99.8% pure, 250 μm thick) in formamide-based electrolyte containing 0.2 M NH_4F and 0.1 M H_3PO_4 at 20 V for 15 h at room temperature (approximately 22°C). After anodization, the samples were rinsed thoroughly with deionized water and isopropyl alcohol, then dried under a stream of nitrogen. Subsequently, samples were crystallized by oxygen annealing at 550 °C for 5h with a heating and cooling rate of 1°C/min.

The morphology of the TiO_2 nanotubes was examined using a field emission scanning electron microscope (FESEM-Zeiss SEM Ultra60). The crystal structure was determined via glancing angle X-ray diffraction (GAXRD) using X'Pert PRO MRD diffractometer with Cu K_α radiation source. The surface properties and composition of the samples were analyzed by X-ray photoelectron spectroscopy using Thermo Scientific K-Alpha XPS with an Al anode. Photoelectrons were collected in hybrid mode over an analysis area of about 1.5 mm^2 by charge referencing the spectra to O 1s at 532 eV.

2.2.8. Solar Cell Assembly and Testing. While in a dry nitrogen environment all samples were immersed in a 0.2 M $TiCl_4$ solution for 45 min at room temperature, then rinsed in ethanol and annealed at 450 ∘C for 45 min. The ruthenium-based complex [Ru (6,6′-(COOEt)2-2,2′-bpy)$_2$(Cl)$_2$] was subsequently infiltrated into the nanotubes using anhydrous ethanol as a solvent. The annealed nanotube samples were immediately immersed overnight in 0.4 mM solutions of the dye. Liquid-junction solar cells were assembled by infiltrating the dye-coated TiO_2 electrode with redox electrolyte containing lithium iodide (LiI, 0.1M), diiodine (I_2 0.01M), tert-butyl pyridine (TBP, 0.4M), butylmethylimidazolium iodide (BMII, 0.6M), and guanidinium thiocyanate (GuNCS, 0.1M) in a mixture of acetonitrile and methoxy propionitrile (v/v=15:1). Conductive glass slides, sputter-coated with 100 nm of Pt, were used as the counter-electrode. The working (nanotubes) and counter (Pt) electrodes were spaced by a 25 μm thick SX-1170 spacer. Photocurrent density and the photovoltage of the dye-sensitized solar cells were measured with active sample areas of 0.4 cm^2 using AM1.5 simulated sunlight

Scheme 1. Stepwise Synthesis of the Complex

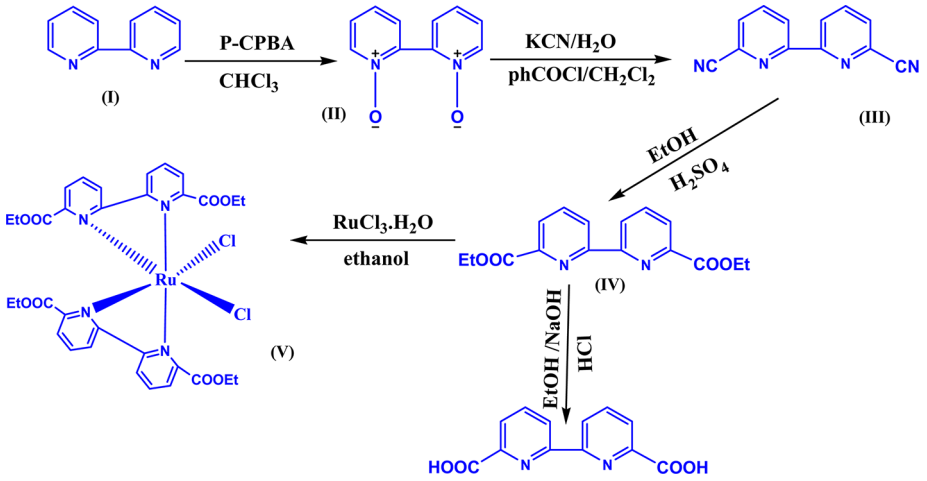

produced by a 50W Oriel Solar Simulator (100 mW cm^{-2}), calibrated with a NREL-certified silicon solar cell, and a CHI 660C potentiostat.

3. RESULTS AND DISCUSSION

3.1. Synthesis and Properties of the Complex. The $[Ru(6,6'\text{-}(COOEt)_2\text{-}2,2'\text{-}bpy)_2(Cl)_2]$ complex was synthesized by a typical one-pot reaction as detailed in the Experimental Section and depicted in Scheme 1. It is worthy to note that the complex was synthesized using Ru $(DMSO)_4Cl_2$ and $RuCl_3$ in water. The ^{1}HNMR spectrum of the crude reaction mixture indicated minimum amount of impurities, which can be probably due to the utilization of a ruthenium(II) precursor with weekly binding ligands (DMSO).

The absorption characteristics and molar extinction coefficient of a dye play a crucial role in deciding the performance of a dye-sensitized solar cell. The electronic absorption spectrum of the complex measured in ethanol is displayed in Figure 1. The complex shows four absorption bands centered at 293, 352, 387, and 500 nm, respectively. According to the absorption profiles, the band at 293 nm is assigned to the overlap of intraligand $\pi-\pi^*$ transitions.[25] Another band centered at 387 nm also contains two components: the $\pi-\pi^*$ transition of the ancillary ligand and one of the metal-to-ligand charge transfer (MLCT) transitions for the complex.[26] The molar absorption coefficient (ε) of the band centered at 500 nm is 1.3 x 10^4 M^{-1} cm^{-1}, which originates from MLCT that is corresponding to transitions from the metal t_2g to the ligand π^*orbital.[27] Table 1 gives the absorption peaks and the corresponding molar extinction coefficients of the synthesized complex and compared to the well-known N-719 dye.

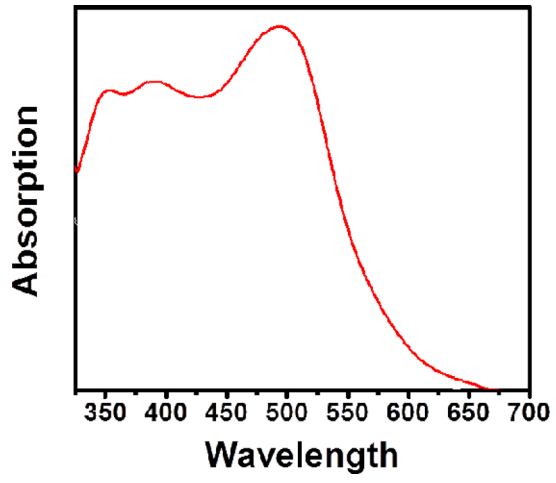

Figure 1. Electronic absorption spectra of 1.8 × 10^{-7} M $Ru(6,6'\text{-}(COOEt)_2\text{-}2,2'\text{-}bpy)_2(Cl)_2$ complex in ethanol.

Note that dichloro complexes are chosen in the current study, instead of the widely used dithiocyanato complexes, due to the strong σ donor property of Cl^- compared to NCS^- ligand.[28] The chloride ligands cause destabilization of the metal t_{2g} orbitals, and raising them in energy relatively closer to the ligand π^*-orbitals resulting in a lower MLCT transition energy. According to Lever, the chloride ligand has a parameter value of −0.24 and the thiocyanate ligand has a value of−0.06.[29] Briefly, a ligand electrochemical parameter (E_L) is a means that allows one to predict the metal-centered redox potential of a variety of complexes on the basis of the additivity of the E_L parameters.[29] This prediction is usually made using the following linear relationship

$$E_{obs} = S_M[\sum E_l(L_i)] + I_M \quad (1)$$

where the slope (S_M) and the intercept (I_M) are constants for all derivatives of a given metal undergoing a defined redox process, i.e., having a defined initial and final oxidation state, coordination number, stereochemistry, and spin state.[29]

3.2. Morphological and Structural Properties of TiO_2 Nanotubes. Figure 2 shows FESEM images of the as-fabricated nanotube arrays. It can be seen that the nanotube array is uniform over the entire substrate. The tubular structure with a nearly uniform wall thickness throughout the length of the tube is evident. The as-prepared samples were found to have a length of approximately 6 ± 0.2 μm, an outer diameter of 85 ± 1 nm, and a wall thickness of 16 ± 1 nm.

After annealing at 550 °C for 5 h in dry oxygen ambient, the pure anatase phase of TiO_2 was obtained as confirmed by GAXRD measurements (Figure 3a). This was also confirmed via XPS analysis (Figure 3b,c) as evidenced by the O1s and Ti2p peaks with the molar ratio Ti/O being close to the stoichiometric proportion. Note also that both Ti $2p_{3/2}$ and $2p_{1/2}$ peaks are observed with a separation of 5.7 eV, which confirms the presence of Ti^{4+}.[30] The above characterizations confirm the synthesized TiO_2 nanotubes to be highly crystalline anatase.

dx.doi.org/10.1021/am301089t | ACS Appl. Mater. Interfaces 2012, 4, 4413−4418

Table 1. Absorption Peaks and Peak Molar Extinction Coefficients of N-719 and Ru-6,6′ Dyes in Ethanol Solutions (λ_{Max} in nm, ε in M^{-1} cm^{-1})

dye	λ_{Max1}	ε_1	λ_{Max2}	ε_2	λ_{Max3}	ε_3	λ_{Max4}	ε_4
N-719	309	46 400	378	11 500	514	11 700		
Ru-6,6′	293	49 000	352	16 000	387	14 000	500	13 000

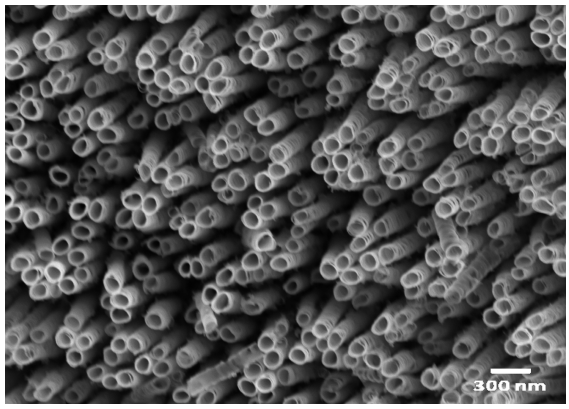

Figure 2. FESEM top-view image of the fabricated TiO_2 nanotube arrays via anodization in formamide electrolytes containing 0.2 M NH_4F and 0.1 M H_3PO_4.

3.3. Solar Cell Performance. The photocurrent (J)−photovoltage (V) performance of an illustrative device, 0.4 cm^2 active surface area, is shown in Figure 4. The nanotube-array DSSC device exhibits a J_{sc} of 8.45 mA cm^{-2}, a V_{oc} value of 0.74 V and a fill factor (ff) of 0.63 to produce an overall conversion efficiency of 3.94%. Note that a maximum power of 3.9 mW cm^{-2} can be delivered at I_{max} = 7.92 mA cm^{-2} and V_{max} = 0.5 V. Despite the limitations of the used device assembly as platinized counter electrode partially reflects light and iodine absorbs photons at lower wavelengths (400−600 nm), the nanotube array based DSSCs exhibit very reasonable V_{oc} and ff compared to those reported for front side illuminated nanocrystalline cells.[31] In such cells, the open circuit voltage is determined by the energy difference between the quasi-Fermi level of the illuminated semiconductor electrode and the potential of the redox couple in the electrolyte.[32]

For n-type semiconductor such as TiO_2, the electrons injection process from photoexcited dye molecules should raise

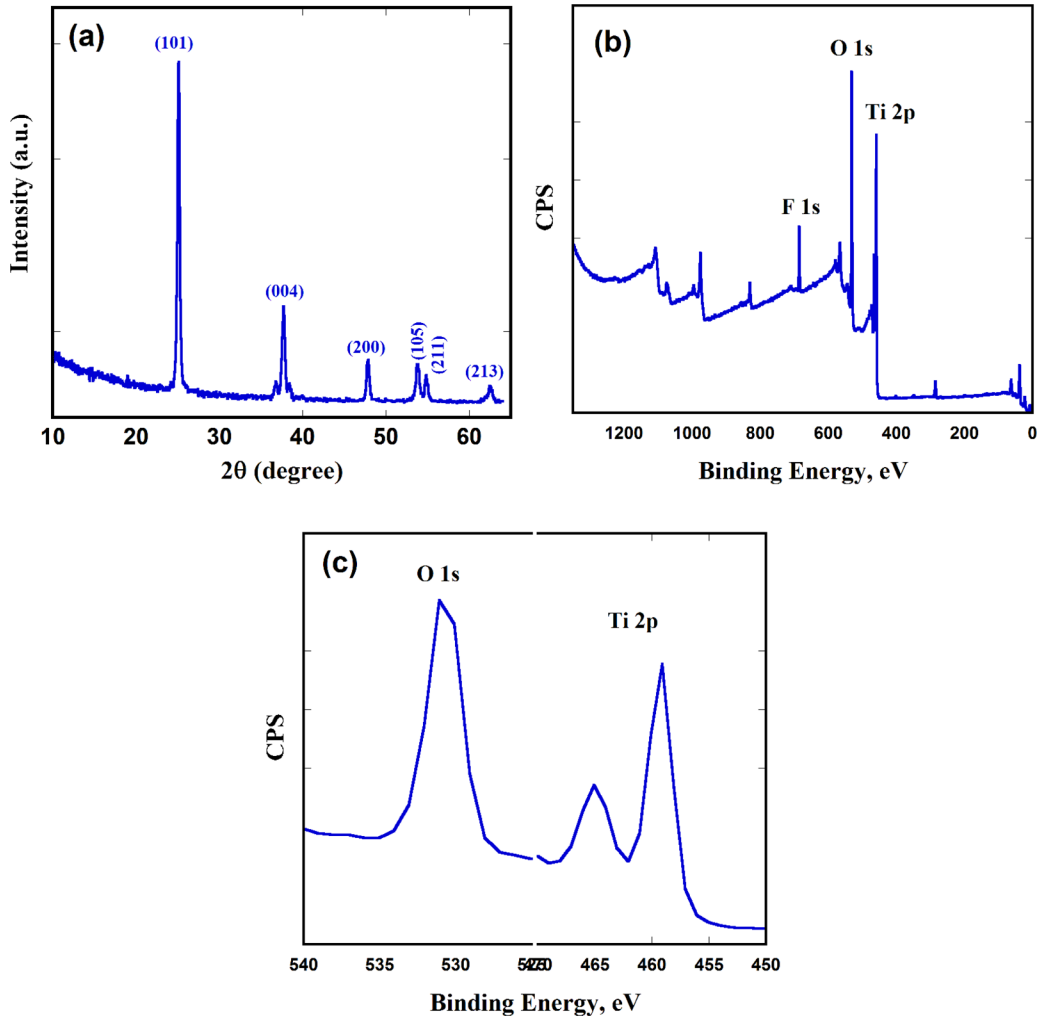

Figure 3. (a) GAXRD and (b, c) XPS spectra of the annealed TiO_2 nanotube arrays.

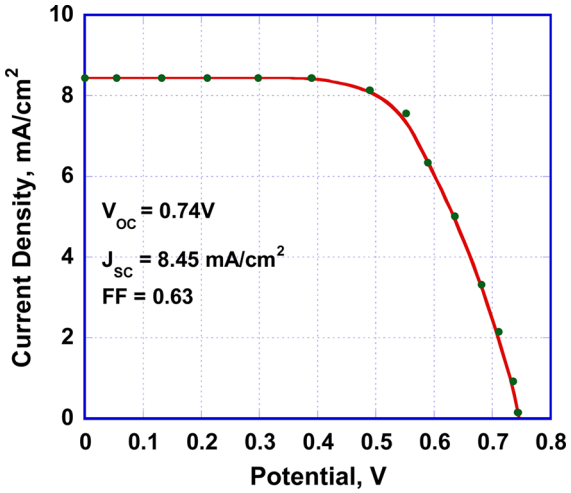

Figure 4. *J*–*V* characteristics of the solar cell device measured under the irradiance of AM 1.5G full sunlight (100 mW cm^{-2}) with a cell active area of 0.4 cm^2.

the quasi-Fermi level towards the TiO_2 conduction band (CB).[33,34] Consequently, the maximum achievable V_{oc} would be equal to the energy difference between the TiO_2 CB edge and potential of the redox (tri-iodide) couple. In this regard, the maximum theoretical value of V_{oc} for n-TiO_2-based DSSCs is 0.95 V.[35] The reported V_{oc} values so far are deviated from the theoretical limit. This deviation is generally related to the interfacial recombination at the TiO_2/electrolyte or TiO_2/dye interfaces.[36] Substantial efforts have been made to overcome such limitations either by coating TiO_2 with a thin layer of insulting metal oxides or by organic molecular additives to the redox electrolyte.[37−39] Under most favorable conditions, V_{oc} values of 700 mV or slightly higher are typically obtained for nanocrystalline TiO_2-based DSSCs using Ru-based dyes.[40] Our obtained V_{oc} of 0.74 V indicates that our newly synthesized dye is comparable to the commercially available ones. The reasonable V_{oc} can, in part, be related to the presence of a thin barrier layer[41] between the Ti metal substrate and the nanotube array, which prevents redox mediators from reaching the back-contact and nearly eliminates the contribution to the dark current from the reduction of the redox mediator at the collector electrode with the oxide layer. On the other hand, the movement of the conduction-band edge of TiO_2 or the suppression of recombination losses[42,43] are two other factors that can be used to account for V_{oc} enhancement. In our device, the superior transport properties of the ordered nanotubular structure[23] may allow for larger electron lifetimes and a suppression of back electron transfer from the electrode to the electrolyte. However, whether the TiO_2 nanotubes have conduction band that is more negative compared to that of nanocrystalline electrodes needs systematic investigation. Another factor that is essential for improvement of the solar cell efficiency is the fill factor (ff), which is reduced with increasing series resistance. Our obtained substantial ff of 0.63 indicates the role played by the nanotube geometry in reducing the series resistance, and hence enhancing the ff. As a last note, it seems that our device components (TiO_2 NTs, dye and redox electrolyte) are working in harmony and that our newly developed dye can replace commercially available ones.

CONCLUSIONS

In summary, by appropriate synthetic methodologies, it has been possible to synthesize a new Ru-based complex derivative (bipyridine-6,6′-dicarboxylate ligand) as well as vertically oriented TiO_2 nanotube arrays. Sensitization of the nanotube arrays (6 μm thick) with the Ru-6,6′ complex enabled the fabrication of a DSSC device that demonstrated a conversion efficiency of 3.94% under the AM 1.5G illumination. The obtained efficiency may suggest the new sensitizer to be a promising candidate for DSSCs applications. Comparison of the obtained open circuit photovoltage of our devices to those published in literature suggests superior electron transport in Ru-6-6′/nanotubular titania-based DSSCs.

AUTHOR INFORMATION

Corresponding Author

*E-mail: nageh.allam@aucegypt.edu.

Notes

The authors declare no competing financial interest.

REFERENCES

(1) Timilsina, G. R.; Kurdgelashvili, L.; Narbel, P. A. *Renewable Sustain. Energy Rev.* **2012**, *16*, 449.
(2) Grätzel, M. *J. Photochem. Photobiol. C* **2003**, *4*, 145.
(3) Ning, Z.; Fu, Y.; Tian, H. *Energy Environ. Sci.* **2010**, *3*, 1170.
(4) Yen, Y.-S.; Chou, H.-H.; Chen, Y.-C.; Hsu, C.-Y.; Lin, J. T. *J. Mater. Chem.* **2012**, *22*, 8734.
(5) Qin, Y.; Peng, Q. *Int. J. Photoenergy* **2012**, *2012*, 291579.
(6) Rack, J. J.; Gray, H. B. *Inorg. Chem.* **1999**, *38*, 2.
(7) Xie, P.-H.; Hou, Y. J.; Zhang, B.W. *J. Chem. Soc., Dalton Trans.* **1999**, 4217.
(8) Argazzi, R.; Bignozzi, C. A.; Heimer, T. A. *Inorg. Chem.* **1994**, *33*, 5741.
(9) Grabulosa, A.; Martineau, D.; Beley, M.; Gros, P. C.; Cazzanti, S.; Caramori, S.; Bignozzi, C. A. *Dalton Trans.* **2009**, 63.
(10) Allam, N. K.; El-Sayed, M. A. *J. Phys. Chem. C* **2010**, *114*, 12024.
(11) Mor, G.K.; Shankar, K.; Paulose, M.; Varghese, O.K.; Grimes, C.A. *Nano Lett.* **2006**, *6*, 215.
(12) Allam, N. K.; Poncheri, A. J.; El-Sayed, M. A. *ACS Nano* **2011**, *5*, 5056.
(13) Kuang, D.; Brillet, J.; Chen, P.; Takata, M.; Uchida, S.; Miura, H.; Sumioka, K.; Zakeeruddin, S. M.; Gratzel, M. *ACS Nano* **2008**, *2*, 1113.
(14) Allam, N. K.; Yen, C.-W.; Near, R. D.; El-Sayed, M. A. *Energy Environ. Sci.* **2011**, *4*, 2909.
(15) Zhu, K.; Neale, N. R.; Halverson, A. F.; Kim, J. Y.; Frank, A. J. *J. Phys. Chem. C* **2010**, *114*, 13433.
(16) Hayden, S. C.; Allam, N. K.; El-Sayed, M. A. *J. Am. Chem. Soc.* **2010**, *132*, 14406.
(17) Zhu, K.; Wang, Q; Kim, J.-H.; Pesaran, A. A.; Frank, J A. *J. Phys. Chem. C* **2012**, *116*, 11895.
(18) Hesabi, Z. R.; Allam, N. K.; Dahmen, K.; Garmestani, H.; El-Sayed, M. A. *ACS Appl. Mater. Interfaces* **2011**, *3*, 952.
(19) Mor, G. K.; Carvalho, M. A.; Varghese, O. K.; Pishko, M. V.; Grimes, C. A. *J. Mater. Research* **2004**, *19*, 628.
(20) Rettew, R. E.; Allam, N. K.; Alamgir, F. M. *ACS Appl. Mater. Interfaces* **2011**, *3*, 147.
(21) Zaban, A.; Greenshtein, M.; Bisquert, J. *ChemPhysChem* **2003**, *4*, 859−864.
(22) Fabregat-Santiago, F.; Garcia-Canadas, J.; Palomares, E.; Clifford, J. N.; Haque, S. A.; Durrant, J. R.; Garcia-Belmonte, G.; Bisquert, J. *J. Appl. Phys.* **2004**, *96*, 6903.
(23) Grimes, C. A.; Mor, G. K. *TiO_2 Nanotube Arrays: Synthesis, Properties, and Applications*; Springer: New York, 2009.

(24) Allam, N. K. *Anodically Fabricated Metal Oxide Nanotube Arrays: A Useful Structure for Efficient Solar Energy Conversion*; VDM Verlag Dr Müller, Dusseldorf, Germany, 2011.
(25) Kalyanasundaram, K.; Gratzel, M. *Coord. Chem. Rev.* **1998**, *77*, 347.
(26) Kohle, O.; Ruile, S.; Gratzel, M. *Inorg. Chem.* **1996**, *35*, 4779.
(27) Kalyanasundaram, K. *Coord. Chem. Rev.* **1982**, *46*, 159.
(28) Haasnoot, J. G. *Coord. Chem. Rev.* **2000**, *200*−*202*, 131.
(29) Lever, A. B. P. *Inorg. Chem.* **1990**, *29*, 1271.
(30) Allam, N. K.; Alamgir, F.; El-Sayed, M. A. *ACS Nano* **2010**, *4*, 5819.
(31) Mor, G. K.; Shankar, K.; Paulose, M.; Varghese, O. K.; Grimes, C. A. *Nano Lett.* **2006**, *6*, 215.
(32) Zhang, Z. P.; Zakeeruddin, S. M.; O'Regan, B. C.; Humphry-Baker, R.; Gratzel, M. *J. Phys. Chem. B* **2005**, *109*, 21818.
(33) Kopidakis, N.; Benkstein, K. D.; van de Lagemaat, J.; Frank, A. J.; Yuan, Q.; Schiff, E. A. *Phys. Rev. B* **2006**, *73*, 045326.
(34) Ni, M.; Leung, M. K. H.; Leung, D. Y. C.; Sumathy, K. *Sol. Energy Mater. Sol. Cells* **2006**, *90*, 2000.
(35) Ogomi, Y.; Kato, T.; Hayase, S. *J. Photopolym. Sci. Technol.* **2006**, *19*, 403.
(36) Kumara, G. R. R. A.; Tennakone, K.; Perera, V.P.S.; Konno, A.; Kaneko, S.; Okuya, M. *J. Phys. D: Appl. Phys.* **2001**, *34*, 868.
(37) Kay, A.; Gratzel, M. *Chem. Mater.* **2002**, *14*, 2930.
(38) Hara, K.; Dan-oh, Y.; Kasada, C.; Ohga, Y.; Shinpo, A.; Suga, S.; Sayama, K.; Arakawa, H. *Langmuir* **2004**, *20*, 4205.
(39) Palomares, E.; Clifford, J. N.; Haque, S. A.; Lutz, T.; Durrant, J. R. *J. Am. Chem. Soc.* **2003**, *125*, 475.
(40) Liu, E.; Aydil, E. *J. Am. Chem. Soc.* **2009**, *131*, 3985.
(41) Allam, N. K.; Grimes, C. A. *J. Phys. Chem. C* **2009**, *113*, 7996.
(42) Niinobe, D.; Makari, Y.; Kitamura, T.; Wada, Y.; Yanagida, S. *J. Phys. Chem. B* **2005**, *109*, 17892.
(43) Frank, A. J.; Kopidakis, N.; van de Lagemaat, J. *Coord. Chem. Rev.* **2004**, *248*, 1165.